Available online at www.CivileJournal.org

Civil Engineering Journal

Vol. 5, No. 11, November, 2019

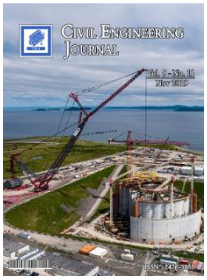

Numerical Investigation of the Behavior of Reinforced Concrete Beam Reinforced with FRP Bars

Rania Salih [a, b*], Zhou Fangyuan [a]

[a] *Huazhong University of Science and Technology, School of Civil Engineering and Mechanics, Wuhan, Hubei 430074, China.*

[b] *Red Sea University, School of Civil Engineering ,Portsudan, Sudan.*

Received 16 July 2019; Accepted 28 September 2019

Abstract

In this study, the behavior of reinforced concrete beams reinforced with FRP bars was investigated. A total of seventeen models were carried out based on the finite element software (ABAQUS). The concrete damage plasticity modeling was considered. Two types of fiber polymer bars, CFRP and GFRP as longitudinal reinforcement for concrete beam were used. The validation of numerical results was confirmed by experimental results, then the parametric study was conducted to evaluate the effect of change in different parameters, such as (diameter size, number of bars), type of FRP bars, longitudinal arrangement for FRP bars. All results were analyzed and discussed through, load-deflection diagram, according, to the difference parameter considered. The results showed that the use of FRP bars in rebar concrete beam improves the beam stiffness and enhance the cracking load. The load capacity enhanced in the range of (7.88-64.82%) when used CFRP bars. The load-carrying capacity of beams strengthened with CFRP is higher than that of strengthened with GFRP. Furthermore, the use of FRP bars in bottom and steel in top reinforcement is useful to overcome the large deflection, and improving the beam ductility. Finally, the results of finite element models were compared with the prediction equation, according to ACI440.1R-15.

Keywords: Reinforced Concrete Beam; FRP Reinforcement; Finite Element Analysis; Load-deflection Curve.

1. Introduction

The use of modern Fiber Reinforced Polymer (FRP) bars for reinforcing and repair structural member (columns, beams, deep beams, and slabs), has been rapidly increased within the past few years. The durability of the reinforced concrete element is a major concern due to the corrosion of steel reinforcement in concrete structures exposed to de-icing salts and marine environments [1, 2]. However, Deficit of mechanical strength of reinforced concrete structures and poor bond behavior between steel and concrete are often caused by the corrosion of steel reinforcement. In addition to a high level of durability and fatigue durability, FRP reinforcing bars have a high strength-to-weight ratio, which creates an attractive choice as reinforcement for concrete structures [3]. The most commonly used in infrastructure and commercially available FRP bars types are included, Carbon fiber reinforced polymer (CFRP), Aramid fiber reinforced polymer (AFRP), Glass fiber reinforced polymer (GFRP) and Basalt fiber reinforced polymer (BFRP). Every type of bars has been different in mechanical properties, physical appearance, and surface configuration. Moreover, FRPs can be produced as bars, ropes, tendons, and grids [4].

* Corresponding author: rania_salih@hotmail.com

http://dx.doi.org/10.28991/cej-2019-03091412

Furthermore, There are many forms of FRP applications, using for strengthening structure, as an external bond, such as FRP sheets and plates which attaching them, to the structure using epoxy or vinyl-ester resin or internally as discontinuous FRP fibers mixed with the concrete, or using near surface mounted technique (NSM) for FRP [5, 6].

Nevertheless, FRPs exhibited brittle behavior and were characterized by their linear-elastic stress-strain response without any obvious yield point. Therefore, FRP bars do not appear ductile like steel reinforcing bars [7]. Furthermore, there is another drawback was pointed through structural engineering viewpoint such as low modulus of elasticity and low shear strength which cause, limited application for FRP bars, consequently, concrete beams reinforced with FRP bars show linear-elastic behavior up to failure without display any yield and their final failure is characterized as brittle whether happens due to FRP rupture or due to concrete crushing; while the latter one can be considered as more advisable for RC flexural structural elements with FRPs [7, 8].

On the other hand, the experimental study conducted in related research, have demonstrated that the longitudinal reinforced beam with carbon and glass FRP and without stirrups have been reduced in shear strength when compared those beam reinforced with same amounts of steel reinforcement [7]. This fact is clear support the relatively low modulus of elasticity of FRP bars. The study also revealed that the axial stiffness of the reinforcing bars is the main parameter in reform the concrete shear strength for flexural members reinforced with FRP bars. To mitigate the shortcomings of FRP bars, a lot of effort has been made to enhance the ductility characteristic of beams reinforced with FRP beam in few research studies, by using hybrid FRP rebar [1]. Harris et al. studied Stress-strain behavior of steel with using hybrid FRP rebar. They showed that inclusion of hybrid FRP bar in reinforced concrete beams causes an important increase in bonding characteristic and the ductility response it was found to be similar in the characteristic of traditional steel bar reinforced concrete beams [8]. However, the complex manufacturing process and high technology used cases a high production cost which results in limited use in the engineering applications of hybrid FRP bars in concrete structures. To optimize the behavior of beam reinforced with FRP bars, there is some methodology was used, such as the addition of steel fibers [9]. It was effective for overcoming the large deflections and crack widths in addition to improving the ductility of the beam. The percentage addition of fiber fraction volume was determined randomly in some experimental work.it was found the ductility index increased by100% when used the additional percentage of fiber 1% [10].

Recently there is a lot of experimental research has been conducted to investigate the behavior of concrete beams reinforced with FRP beams. Particularly for GFRP, It has reported that GFRP reinforced beams experience higher deflections and larger crack widths when compared to traditionally reinforced beams with steel bars [11-13]. In addition, the low post cracking and flexural stiffness have been exhibited with these beams. This is due to low modulus of elasticity GFRP which documented in ACI440-15 it can be concluded that the behavior of reinforced concrete beam reinforced with FRP bars under a different type of loads needs to investigate with analytical, experimental and numerical, research [14].

In this study, the finite element modeling was used to investigate the behavior of reinforced concrete beam, reinforced by FRP bars. Two types of bars were used, CFRP and GFRP with normal strength of concrete grade (25, 30, 45) MPa. CFRP bars were used for tension reinforcement while the GFRP were used for tension and compression. The finite element modeling is validated using the previous experimental results conducted by Karayannis et al. (2018) and Adam et al. (2015) [15, 16]. The parametric study was included here to investigate the effect of type FRP, number and size of bars and grade of concrete compressive strength.

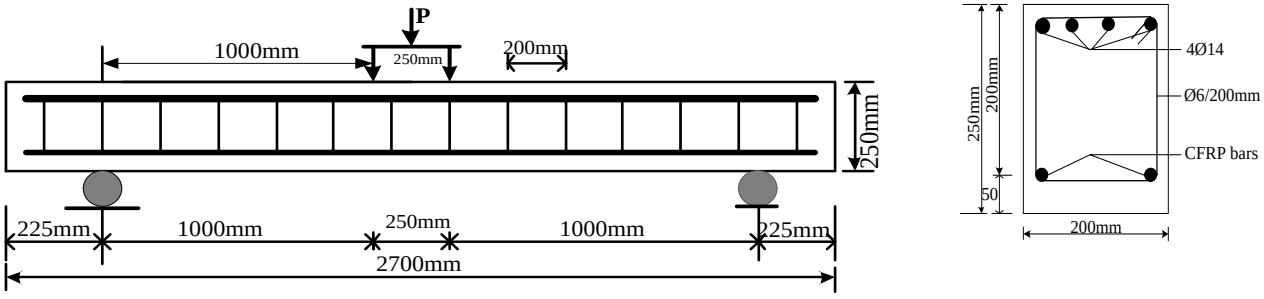

(a) beam tested by Karayannis et al. (2018), denoted Exp1

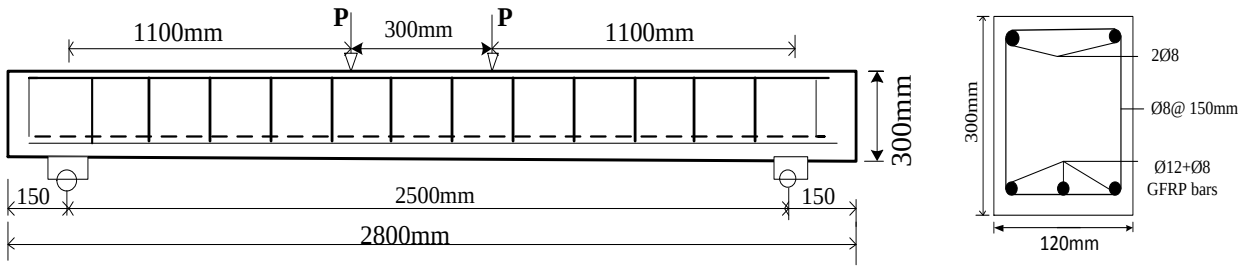

(b) Beam tested by Adam et al. (2015), denoted Exp2

Figure 1. Dimension and details of experimental beams (Exp1, Exp2) [15, 16]

2. Finite Element Modeling

In order to accurately modeling all components of the concrete beam, steel bars, FRP bars, and stirrups were considered and simulated properly. Meanwhile, material properties, nonlinear boundary conditions, and element meshing were concentrated inbuilt the model to get accurate results [2]. The simulated models have used the experimental work for a reinforced concrete beam which conducted by Karayannis et al. (2018) [15] and Adam et al. (2015) [16]. The two studies were used fiber polymer bars, CFRP and GFRP respectively, and were tested under four-point load. Every reinforced concrete specimen has a different amount of reinforcement, a diameter of bars and grades of concrete compressive strength. The dimension and detail of specimens were shown in Figure 1. The following sections hold some details of the FE modeling procedure. The simplified steps for beam modeling by use Abaqus software as shown in Figure 2.

2.1. The Establishment of Model

The first simply supported beam is 2700 mm long; with a rectangular section of 200×250 mm. the Concrete strength is C30, Longitudinal reinforcement of steel, CFRP and stirrups and the second beam with long 2800mmm with cross-section of 120×300 mm; the Longitudinal reinforcement of steel, and GFRP the Concrete strength is C25, C45 adopted as seen in Figure 1. In ABAQUS, the concrete adopted C3D8R element and the reinforced used T3D2 element. The element is capable of plastic deformation and damaging form [17]. The definition of the plastic deformation stage for the material is different, reinforced enter its plastic stage stress-strain relationship. The Concrete Damaged Plasticity was considered.it can be used for static loading, cyclic loading, and dynamic loading and so on, and has good convergence. The Embedded technology was used to define frictional contact between concrete material and reinforcement cage (steel, FRP, stirrups).

2.2. The Material Properties

The material property for all beams component with the same detail in pre-experimental work was considered. In all cases, the nonlinear linear isotropic stress-strain relation was used for model concrete in compression. Several compression models for concrete have been developed in the predecessor research. Hognestad model has been used in this study, by the numerical expression Equations 1 and 2 [18].

Truss elements (T3D2) was used to model the longitudinal and transverse FRP reinforcements. The item is also having capable of plastic deformation, for general practice, the elastic-plastic model is mostly used with or without the use of strain hardening. The steel reinforced had a200GPa modulus of elasticity, and 0.3 for poison's ratio. Whereas the ultimate tensile strength of CFRP and GFRP is1800 MPa, 640 MPa, respectively. And the elastic modulus was used is 130GPa for CFRP, and 40GPa for GFRP.

$$\sigma = \begin{cases} f_c\left[2\frac{\varepsilon}{\varepsilon_0} - \left\{\frac{\varepsilon}{\varepsilon_0}\right\}^2\right] \\ f_c\left[1 - 0.15\frac{\varepsilon - \varepsilon_0}{\varepsilon_\mu - \varepsilon_0}\right] \end{cases} \quad \text{Where} \quad \varepsilon \le \varepsilon_0, \quad \varepsilon_0 \le \varepsilon \le \varepsilon_\mu \tag{1}$$

$$\sigma = \begin{cases} f_t \left[1.2 \frac{\varepsilon}{\varepsilon_0} 0.2 \left\{ \frac{\varepsilon}{\varepsilon_t} \right\}^6 \right] \\ \frac{\varepsilon}{\varepsilon_t} \\ f_t \frac{\frac{\varepsilon}{\varepsilon_t}}{a_t \left(\frac{\varepsilon}{\varepsilon_t} - 1 \right)^{1.7} + \frac{\varepsilon}{\varepsilon_t}} \end{cases} \quad \text{Where } \varepsilon \le \varepsilon_t, \ \varepsilon > \varepsilon_t \tag{2}$$

Where f_c, f_t is compressive and tensile strength, ε_0, ε_u is yield and ultimate limit strain.

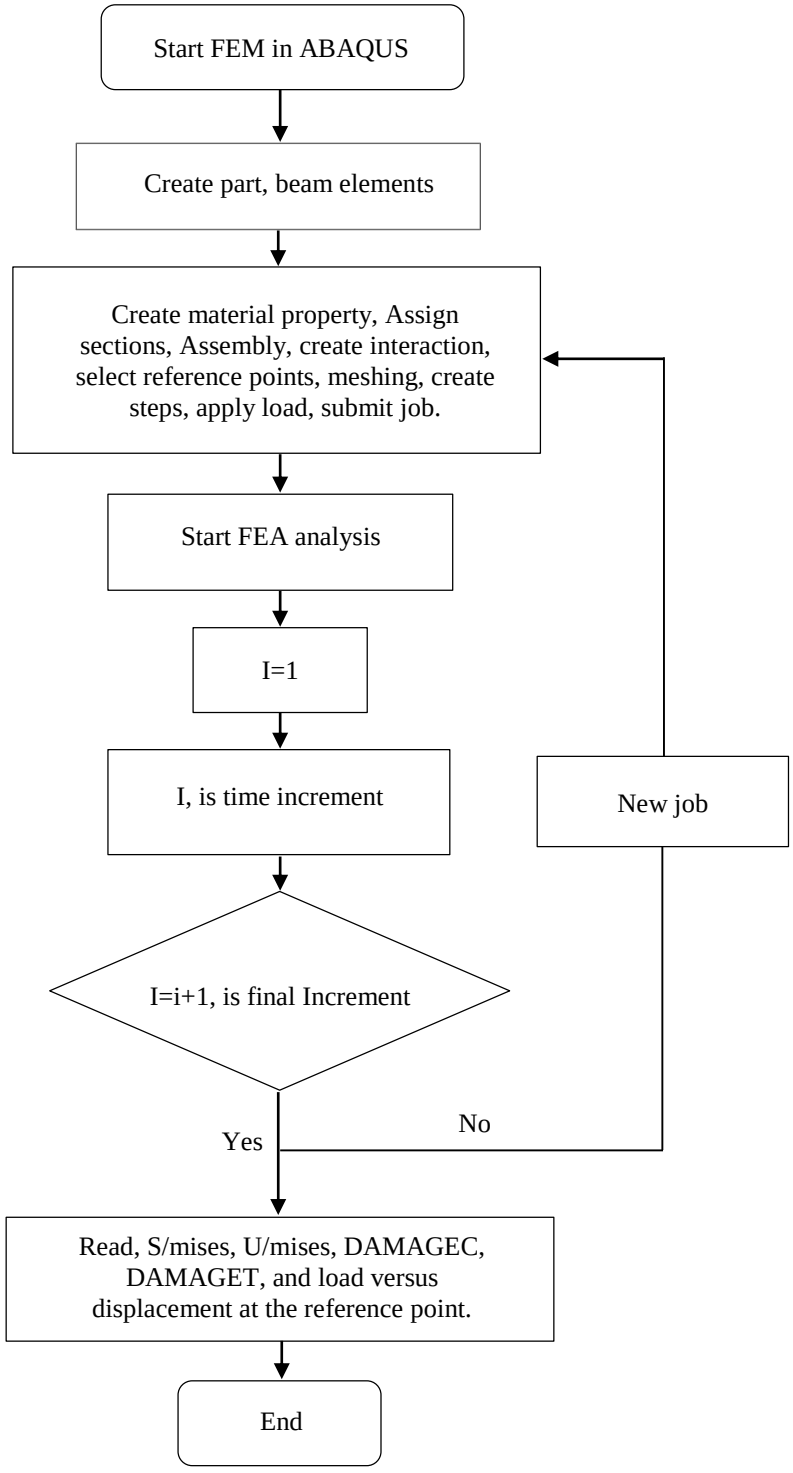

Figure 2. Flowchart for beam modeling in Abaqus

2.3. The Failure Model Condition

In ABAQUS, the model is capable of predicting the failure of concrete; it was defined directly using concrete damage plasticity for material properties. The process of damage can be attributed to micro- cracking, starting on beam section, and increase wider and then coalescence until failure occurs. The plasticity behavior can be characterized by several phenomena such as strain softening, gradual deterioration, and volumetric expansion, etc. which causes the reduction in strength and stiffness of concrete. Damage is usually characterized by the degradation of stiffness. It is assumed that the failure mechanism is related to two factors, are the tensile cracking and compression crushing of the concrete material. ABAQUS program requires the plastic stress-strain for concrete damage, the numerical expressions Equations 3 and 4, were used along Equation 5, Proposed model by Lubliner et al. (1989) to evaluate plastic-damage when degradation occurs only in the softening range and the stiffness is proportional to the cohesion of the material [19].

$$\frac{\mathrm{E}}{\mathrm{E}_0}=\frac{C}{C_{\max}}=1-d \tag{3}$$

$$\bar{\varepsilon}^{p}=\varepsilon^{p}-\frac{d}{1-d}\frac{\sigma}{E_0} \tag{4}$$

$$\bar{\varepsilon}^{p}=\varepsilon-\frac{f}{\mathrm{E}_0} \tag{5}$$

Where c is cohesion in the yield criteria, which is proportional to stress; and c_{max} is equivalent to the strength of the concrete, d is a damage factor. Which f is either the tensile or compressive strength of concrete, can be related to the damage factor d as $\bar{\varepsilon}^{p}$.

2.4. Meshing and Loading Boundary Condition

In order to obtain reasonable convergence and accurate result of modeling for concrete beam reinforced with a different type of FRP bars. The element mesh sizes were selected carefully to achieve a robust result in reasonable computation time. Mesh element for concrete is 3D solid, which is called C3D8R, and for the steel and FRP, it is 2D truss, which is called T3D2 [20]. The model considers loading conditions in term of general static. For all models, loading point was located at the top center of the beam (reference point) and displacement and was computed by defining a node (defined a set in ABAQUS) at the bottom center of the beam. In addition, the loading conditions were assigned and applied on the top of the plate in the same recommended in testing concrete by defining a load-displacement control parameter and corresponding loading rate. Reference Point (RP) is set for all loadings and support's reactions. The bottom supports are hinge which the degree of freedom of U1, U2, and U3 has considered zero and the ends of the beam are pinned in order to avoid rotation of the beam. The atypical figure of 3D mesh beam elements is shown in Figure 3.

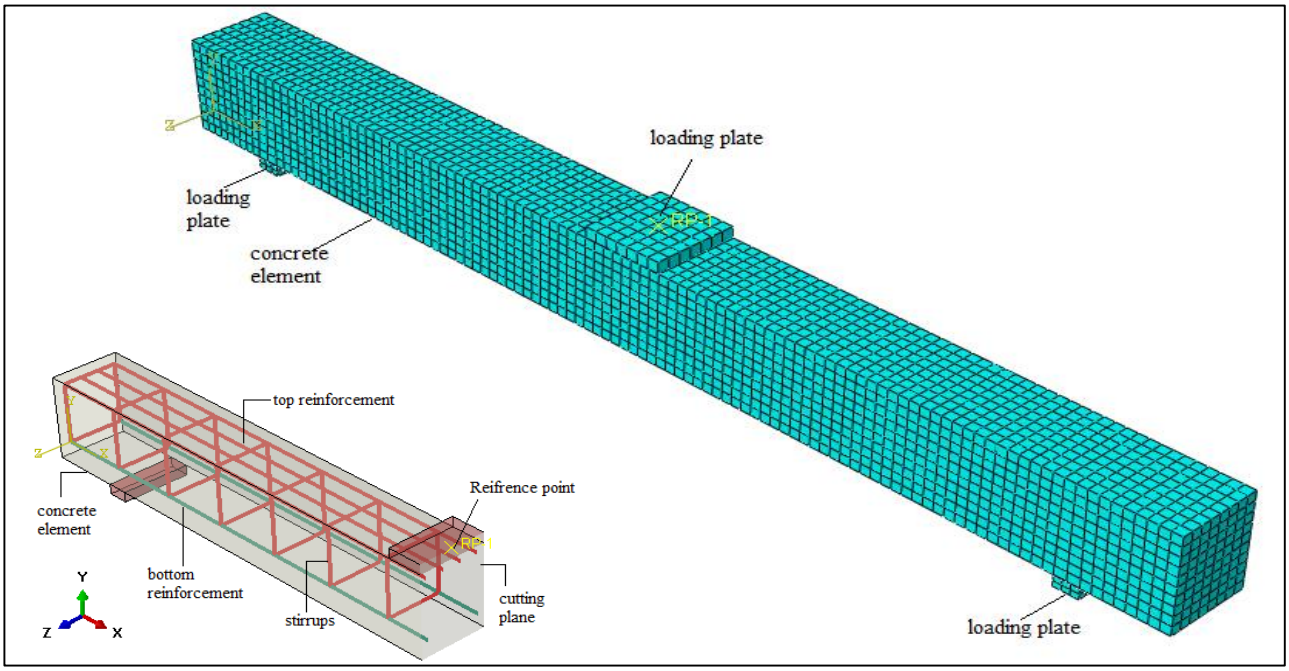

Figure 3. The typical figure of 3D FE mesh (concrete element steel and FRP reinforcement)

2.5. Finite Element Modeling Verification

To validate the finite model, a comparison study with published experimental results was done. Verification of FE results passes through a gradual path. The first step consists of modeling for simply supported beam reinforced of steel bar with geometry details was shown in Figure 1. The applied load and corresponding maximum deflection at mid-span were got. The second step is comparing the FE result with experimental through the load-deflection curves, as shown in Figure 5. For the analysis of the result of Mises stress for beams as shown in, Figure 4-a. The maximum of stress appears in the support and around the loading plate also appears greater stress, changing from max- to min. Similar to the arched truss force model of the beam with web reinforcement, the stress distribution between two supports forms Stress arch. Since the force of beam shoulder is small, Mises stress is lower, and Mises stress in the bottom of the beam is lower under the effect of reinforcement (FRP) See Figure (4-b). For the same caseload, the displacement of nodes in the middle and its time variation is shown in Figure (4-c). The result appears, with the increase of calculation time, span deflection growth gradually accelerated. Since reinforced concrete in the elastic phase have high strength and strong rigidity, the amount of change in mid-span of deflection is small in the beginning; after entering the plastic stage, the material property of reinforced concrete declines, and therefore the acceleration of the deflection of the beam speeds up, thereby forming an acceleration in the mid-span deflection curve. This shows that the simulation is of a reliable theoretical basis, very credible. In addition, the cracks and failures pattern as shown in Figure (4-d), is a good agreement with experimental results.

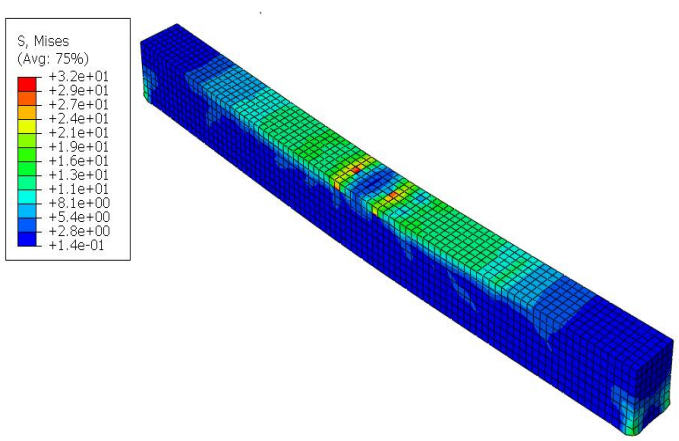

(a) Normal stress of beam reinforced with CFRP bar

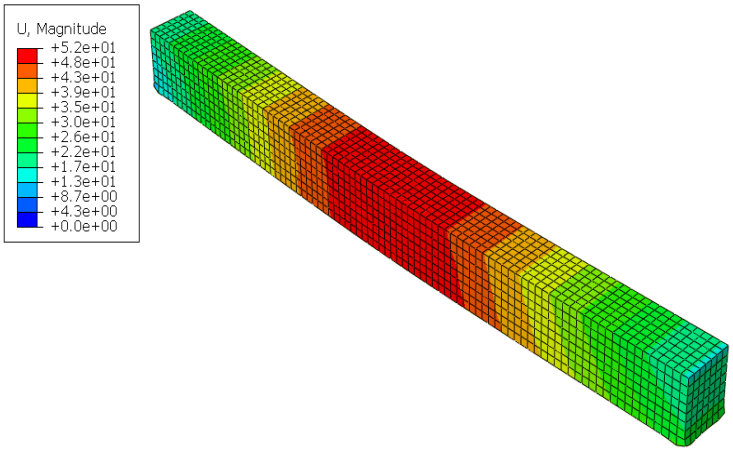

(b) Ultimate deflection of beam reinforced with CFRP bar

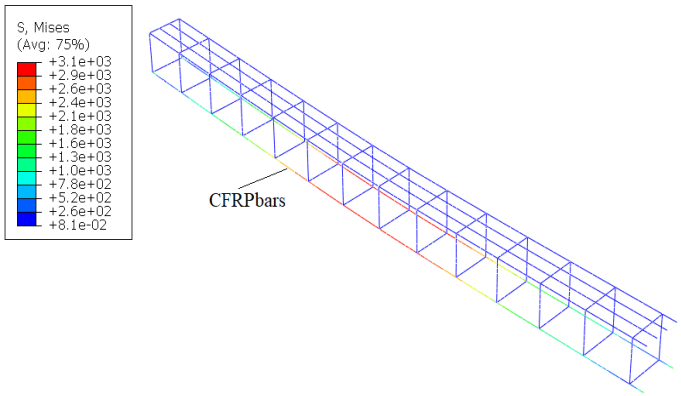

(c) Normal stress for reinforcement cage (steel, CFRP, stirrup)

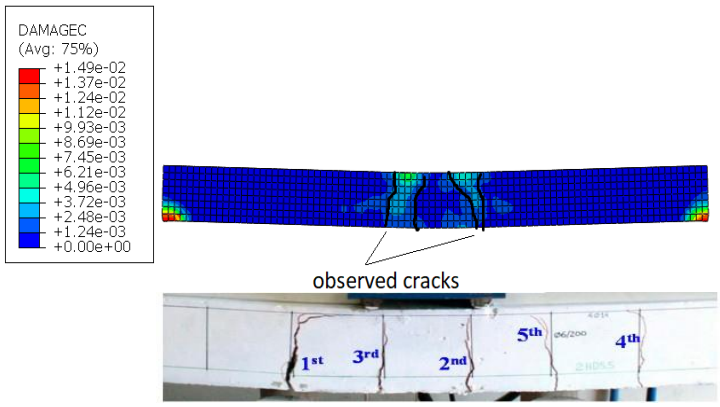

(d) Cracks and damage pattern

Figure 4. finite element models result (beam with FRP reinforcement)

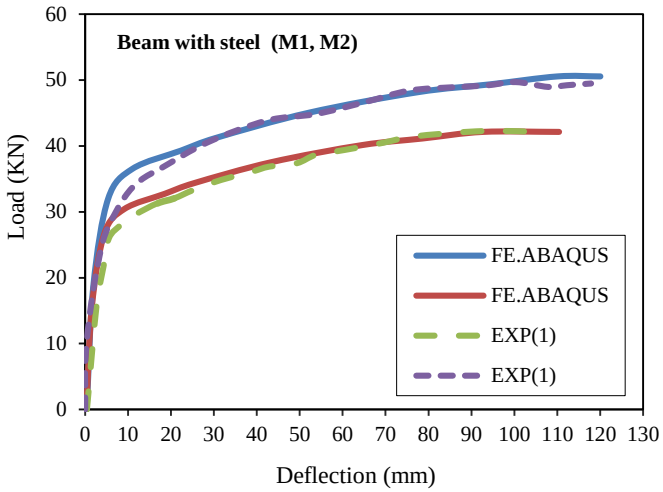

(a) Load-deflection curve

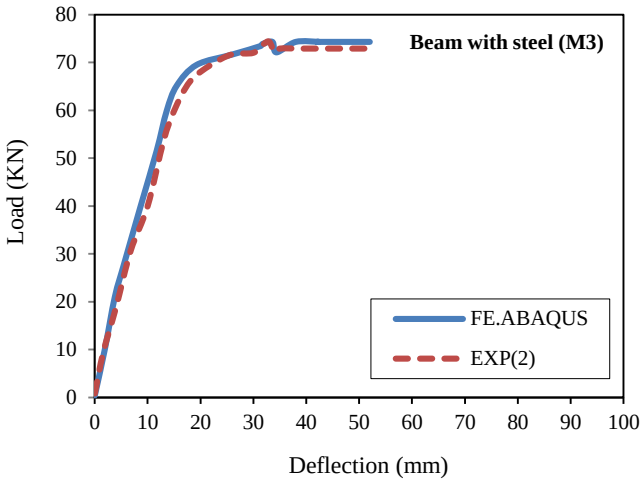

(b) Load-deflection currve

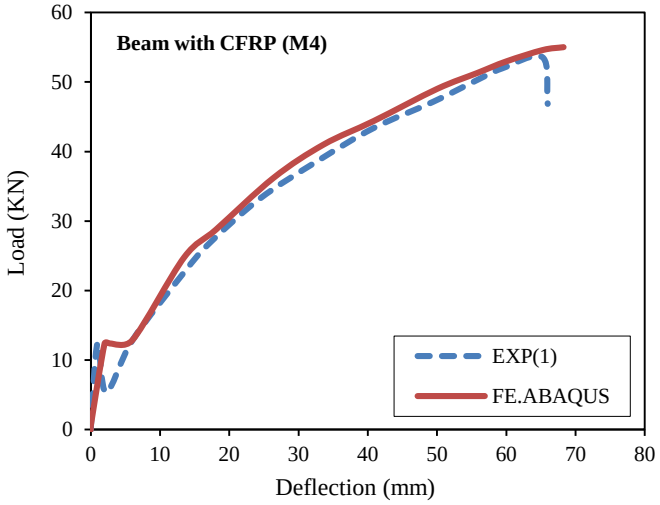

(c) Load-deflection curve

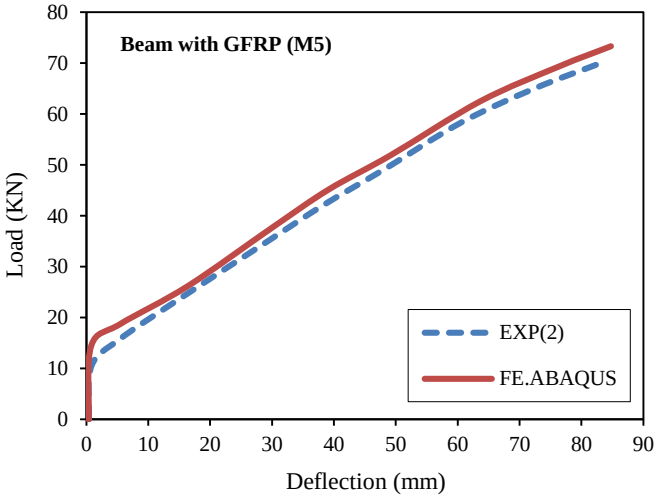

(d) Load -deflection curve

Figure 5. beams with deferent type of reinforcement (Steel, CFRP, GFRP)

3. Parametric Study

A total of 17 models were used, same scaling, loading pattern and material properties followed from exp1 and exp2 for valid finite element program and then for parametric study, to study the behavior strength of beam reinforced with FRP bars. The models were divided into three groups (1, 2, and 3). The models have been different in the type of fiber, the diameter of bars, reinforcement arrangement, and grade strength of concrete. Group (1) contain (M1, M2, M3, M4, M5) with pure steel in the top and bottom reinforcement for control beams, and CFRP, GFRP bars for other beams, as detail in the Table 1 this group was used for verification of finite element models. All specimens in group (2) were reinforced with CFRP bars for tension reinforcement, while the group (3) consist of GFRP reinforcement on top and bottom of beams. Both groups (2) and (3) was used for parametric study. Group (2) contains the models from M6 toM11 strengthened with CFRP as details in Table 1.The steel was used in the top, (fixed diameter bar) and CFRP in the bottom with variation in number and size of bars. The high size of steel in compression reinforcement zone has been used in experimental work, in order to avoid premature failure. In addition, there is some specimens have an anchorage system of CFRP bars was fixed at the support of the beam to improve bond properties. However, this application of spiral length was ignored in modeling, but there no effect in model results. Group (3) contains the models from M12 to M17. All beams were reinforced with GFRP bars as details in Table 1. The fiber bar was used for top and bottom (compression, tension) for beam; the main parameter was used, the number and size of fiber bar (reinforcement ratio) and concrete compressive strength.

Table1. Details of studied parameters

Group	Model	detail of reinforcement			
		Top	Bottom	Notes	Stirrups
1	M1	4Ø14	2Ø10	steel	Ø6@200
	M2	4Ø14	2Ø12	steel	Ø6@200
	M3	2Ø8	1Ø12+1Ø8	steel	Ø8@150
	M4	4Ø14	2HD5.5	steel +CFRP	Ø6@200
	M5	2Ø8	2Ø12+1Ø8	GFRP	Ø8@150
2	M6	4Ø14	2Ø5	steel +CFRP	Ø6@200
	M7	4Ø14	2Ø6	steel +CFRP	Ø6@200
	M8	4Ø14	3Ø6	steel +CFRP	Ø6@200
	M9	4Ø14	2Ø10	steel +CFRP	Ø6@200
	M10	4Ø14	2Ø12	steel +CFRP	Ø6@200
	M11	4Ø14	3Ø12	steel +CFRP	Ø6@200
3	M12	2Ø8	2Ø8	GFRP	Ø8@150
	M13	2Ø8	1Ø12+1Ø8	GFRP	Ø8@150
	M14	2Ø8	2Ø12+1Ø8	GFRP	Ø8@150
	M15	2Ø8	1Ø12+1Ø8	GFRP	Ø8@150
	M16	2Ø8	2Ø12+1Ø8	GFRP	Ø8@150
	M17	2Ø8	4Ø12	GFRP	Ø8@150

4. Results and Discussion

Figure 6 shows grouped load-deflection curves for molded beam, which reinforced with CFRP, the load-deflection curve exhibit a Bi-linear response, which consists of two-part. The first part explains the untracked beam section, in this part the flexure stiffness of the beam is high, and while the second part reflects the load-deformation response represented the cracked stiffness of the beam. After the cracking part, the stiffness of the beam becomes lower, with an increase of load the steel bar was yield and CFRP bar rupture until failure was reached.

When analysis the result, for modeled beam in the group (2) through Figures 6-a, 6-b, and 6-c, it was apparent that there is a significant increase for beam capacity with increase the size and number of CFRP bars. the increase of ultimate load capacity of the beam by 7.88% compared series A models (M6, M7, M9) to the control beam average load capacity from (M1, M2).In the series B model (M9, M10, M11), beam capacity increased by 64.82% compared to the controls beam. It can mention from the series A, B modeled beams with CFRP ensure improving in stiffness and desirable ductile flexural behavior of the beam. This is due to increase in number and diameter of CFRP bars. Besides the high number of steel bar in compression zone contribute to the flexibility of the beam. This better performance is due to arrangement repair the top of the beam with a steel bar and bottom with of CFRP bar.

Figure 7 shows load-deflection curves for molded beam reinforced with GFRP, the first part of the curve reflect the uncracked level for beam which they have high stiffness. It can determine the value of loading required to produce the cracking. The average initial cracked load of series A (M12, M13, M14) is 11.66 and 17.33 kN for series B models (M15, M16, M17). The compressive strength was used is 25 and 45 MPa for series A and B of models respectively. This attribute for concrete grade strength. The ratio of average cracking load for series B two to A is 1.488 this is close for the ratio of the square root of compressive strength 45 to 25 is 1.34 this similar in experimental work was done.

To analyze the result from all models in group (3) through the load-deflection curve Figure 7-a and 7-b, the behavior of GFRP reinforced concrete beams were compared to the behavior of control beam (M3) as shown in Figure 7-c. The load capacity of the reinforced beam with a change in diameter and number of bars was considered, in addition to the compressive strength of concrete, produces little increase in overall stiffness. Figure 7-c shows, beam stiffness reduction by 27.73% for series A models (M12 M13, M14), but increased by 10% compared series B models (M15, M16, M17) to the control beam. Both series A, B beam exhibited greater mid-span deflection than control beam. This attributed to the small value of GFRP modulus elasticity.it was notice the improvement in the capacity of beam is related for both the replacement of steel bars to GFRP bars, an increase in compressive strength of concrete.

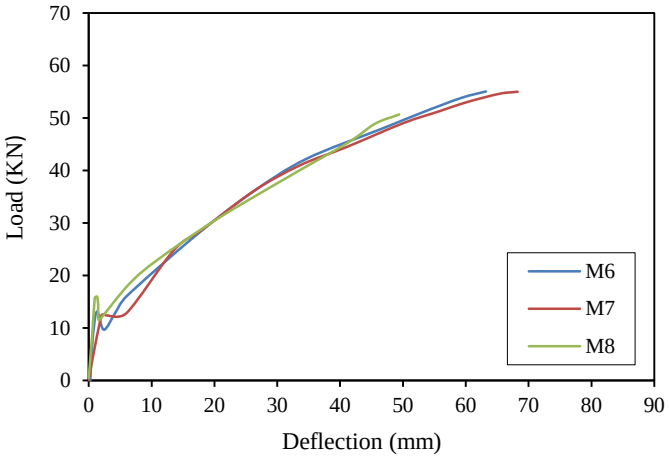

(a) Series A-group1

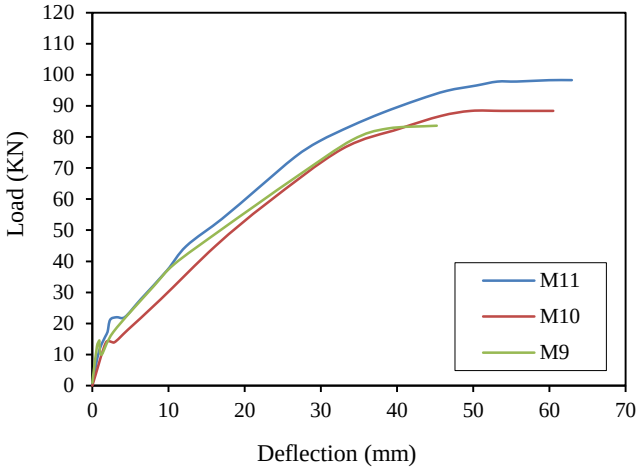

(b) Series B group1

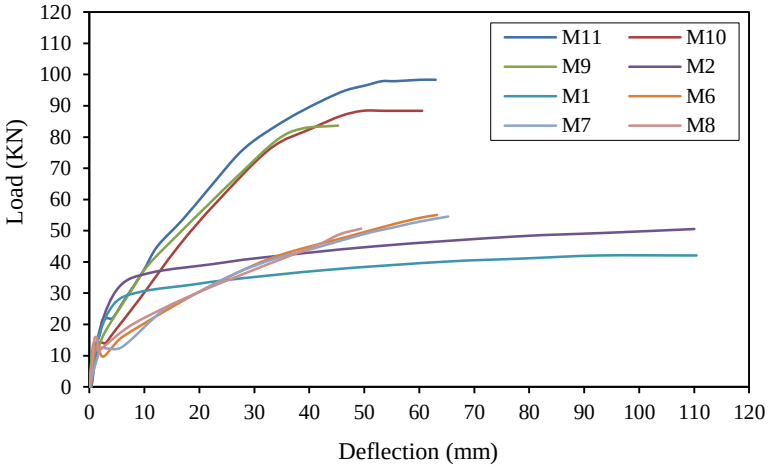

(c) Series A, B, and M1, M2

Figure 6. load-deflection curve of beams with CFRP (group (1) models)

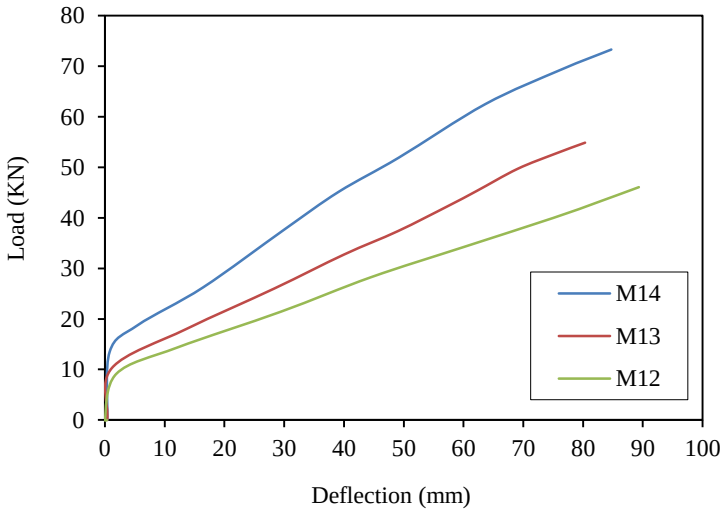

(a) SeriesA-group2

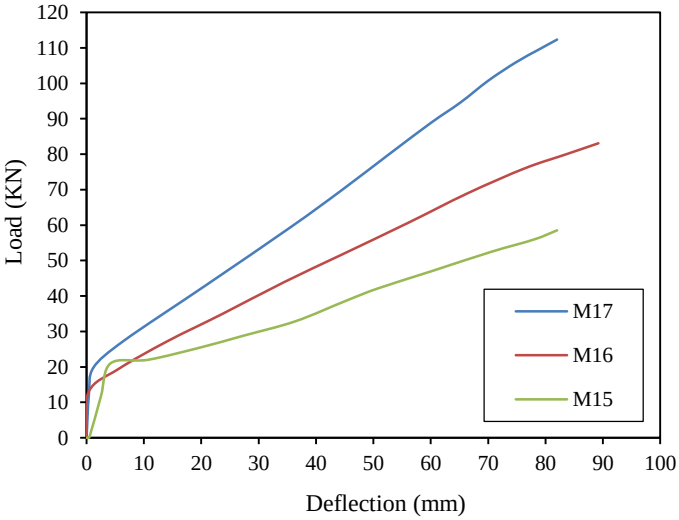

(b) SeriesB-qroup2

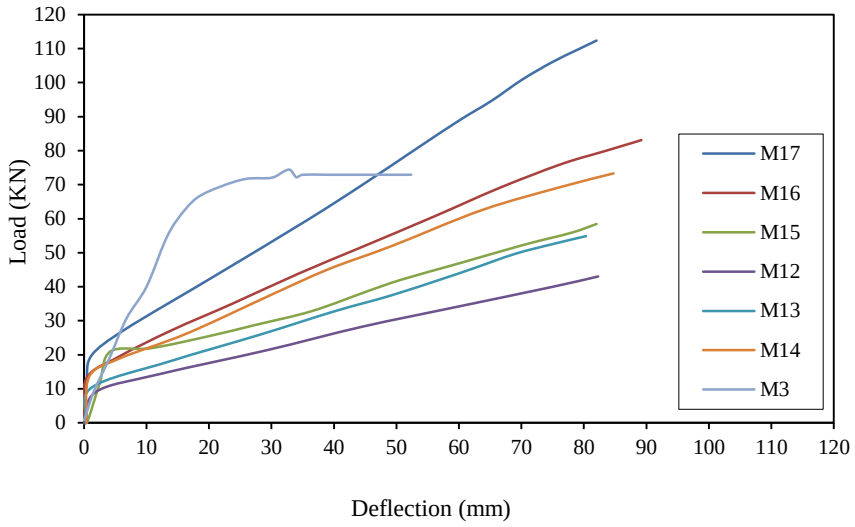

(c) SeriesA,B andM3

Figure 7. The load-deflection curve of beams with GFRP (group (2) models)

5. Theoretical Study on Service Deflection

Owing to the low modulus of elasticity of the FRP bars, the design requirement of concrete beams reinforced with FRP bars are typically estimated by the serviceability limit state. Therefore, a calculation method for predicting the deflection of concrete beams reinforced with FRP bars is needed. ACI 440.1R-06, and ACI 440.1R-15 [14] suggests that the effective moment of inertia can be calculated by Equation 6.

$$I_e = \frac{I_{cr}}{1-\gamma\left(\frac{M_{cr}}{M_a}\right)^2\left(1-\frac{I_{cr}}{I_g}\right)} \le I_g \quad Where \quad M_a \ge M_{cr} \tag{6}$$

Where I_e is the effective moment of inertia, I_{cr} is the moment of inertia of the cracked section I_g is the moment of inertia of gross section, M_{cr} is the cracking moment, M_a is the applied moment γ is the factor $(1.72\text{-}0.72(M_{cr}/M_a))$ which is related to the loading and boundary condition.

ACI 440.1R-15 [14] assumes that before the cracking of the concrete, the section is homogeneous and the contribution of reinforcement to the moment of inertia of the gross section is can be negligible. The moment of inertia of the gross section I_g, can be calculated by Equation 7.

$$I_g = \frac{bh^3}{12} \tag{7}$$

Where b is the breadth of the beam, h is the total depth of the beam. ACI 440.1R-15 [14], assumption that the concrete contribution in the tension zone can be neglected after the cracking of the concrete, the moment of inertia of cracked section can be calculated by following expression Equations 8 and 9.

$$I_{cr} = \frac{b}{3}d^3k^3 + n_f A_f d^2(1-k)^2 \tag{8}$$

$$k = \sqrt{2\rho n_f + (\rho n_f)^2} - \rho n_f \tag{9}$$

Where d is the distance from the maximum compression fiber to the centroid of tensile reinforcement, n_f is the modulus ratio between the FRP bar E_f and the plain concrete E_c, ρ is the reinforcement ratio ,k is factor depend on reinforcement ratio used.

To comparison, the calculation method developed by modeling result in this work, the service load deflections of the modeled beam were calculated by Equation 10 considering the second moments of area calculated by the recommendations in current ACI 440.1R-15.

$$\delta = \frac{PS}{48E_c I_e}\left(3L^2 - 4S^2\right) \quad (10)$$

Where δ is the deflection, P is the applied load, L is the length of the beam, and S is the shear span beam.

Comparison of the modeling result with analytical predictions according to ACI440.1R-15 are presented in Figure 8.

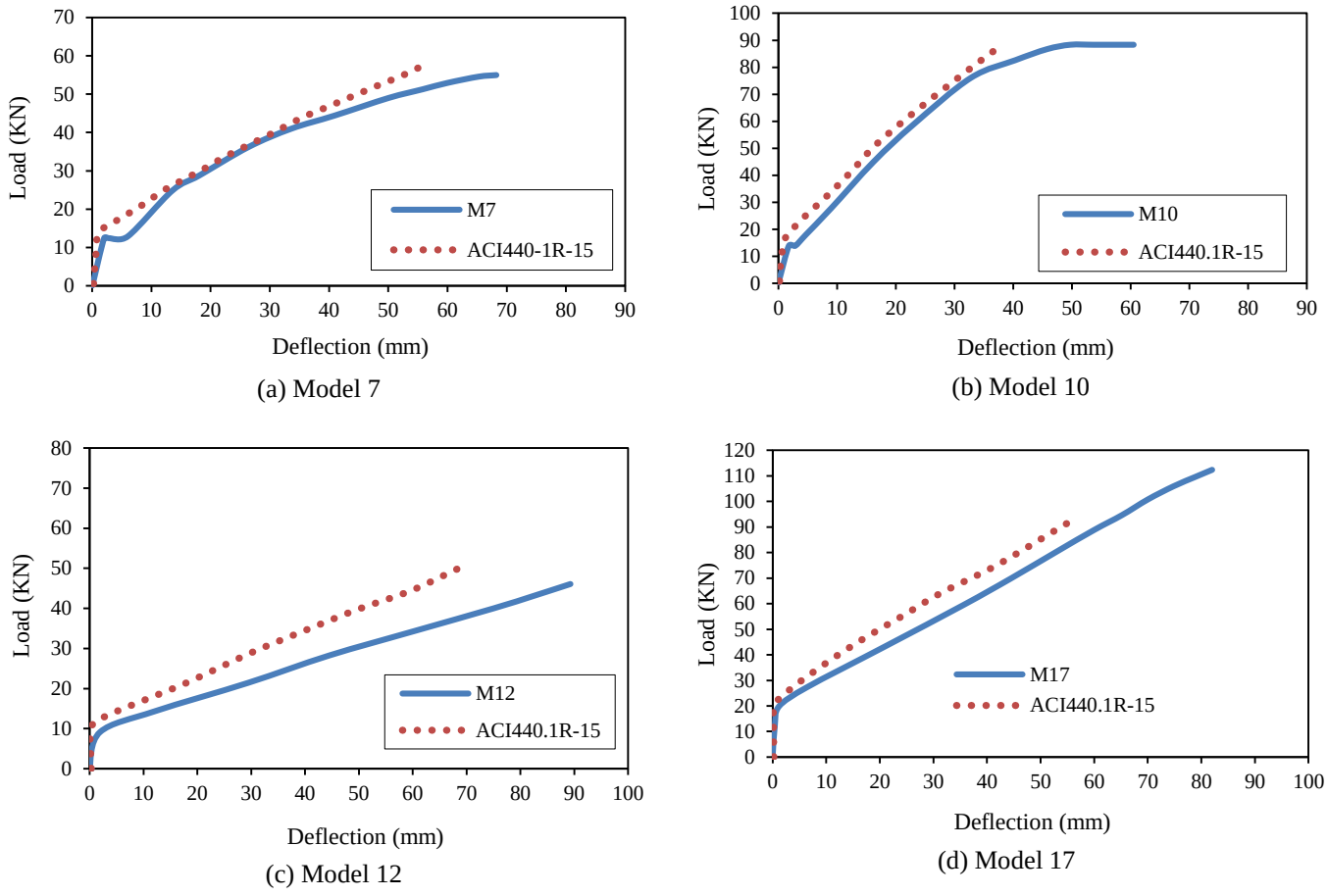

Figure 8. Comparison of the models results with predictions according to ACI440.1R-15

6. Conclusions

This study investigated the behavior of reinforced concrete beam, reinforced with FRP bars, based on finite element analysis software (ABAQUS). To validate modeling, the experimental work from previous studies was used. A parametric study and compare the results of modeling with theoretical prediction according to current ACI440.1R was done through comparison of different graphs. The general conclusion for this study is outlined below.

- The results of the finite element modeling are agreed with an experimental study conducted from previous literature. Addition to comparing the simulation results with analytical predictions, which ensure accuracy and consistency of ABAQUS in investigating the behavior of reinforced concrete beam reinforced with FRP bars.
- As in the experimental work result, the modeling results confirm the use of FRP bars in bottom repair or a total replacement for traditional steel reinforcement improves the beam stiffness through compare beams with the control beam. A good agreement between the finite element modeling result and experimental in term of loads carrying-capacity, deflection at mid-span, In addition to the failure pattern.
- The result of several models for both types of CFRP and GFRP bars as main reinforcement for concrete beam indicates the effective of FRP system with an increase in the amount reinforcement (number, size bars). Improve in-service load due to the high strength of FRP and increase the deflection as attributes of low elastic modulus. The upgraded in load capacity with used CFRP bars, the beam exhibited higher capacities in range (7.88-64.82%), while not more than 10% for GFRP. The load carrying capacity of beams strengthened with CFRP is higher than that of strengthened with GFRP.

- The beneficial effect of CFRP bars was clear when changing the small diameter bars to bit large with the same number of bars. The load carrying capacity increased by 51.85% with notice of no change in deflection.
- The change of reinforcement amount (size, number) for GFRP bars has not effective in load carrying capacity, without an increase in compressive strength of concrete. The first crack load increases by48.62% when increasing the concrete compressive strength in the order of 25Mpa to 45Ma.
- Through the bi-linear load-to deflection curve for CFRP, the increase of bars tend to some ductility of the beam, on the other hand, there is no noticeable ductility provides with GFRP bars repairs in the form (top-bottom) reinforcement. This regard to two reasons, first contributes to the low-value of modulus of elasticity for GFRP compare the CFRP, second for the form of use top-bottom for GFRP while CFRP as the bottom. It can be concluded the better to use steel bars as top reinforcement with FRP bars as bottom reinforcement of concrete beam.
- The general observation from the comparison the finite element results with the prediction equation according to current ACI440.1R code. Show that the code provisions for the estimate the load to deflection relation of FRP reinforced concrete beam is very conservative. For more accurate to predict the behavior of beam with use codes provision a lot of comparisons was needed for future work.

7. Conflicts of Interest

The authors declare no conflict of interest.

8. References

[1] Benmokrane, Brahim, Michele Theriault, Radhouane Masmoudi, and Sami Rizkalla. "Effect Of Reinforcement Ratio on Concrete Members Reinforced with FRP Bars." Evolving Technologies for the Competitive Edge. 42 (1997): 87-98.

[2] Mustafa, Suzan A.A., and Hilal A. Hassan. "Behavior of Concrete Beams Reinforced with Hybrid Steel and FRP Composites." HBRC Journal 14, no. 3 (December 2018): 300–308. doi:10.1016/j.hbrcj.2017.01.001.

[3] Thamrin, Rendy, and Tetsuzo Kaku. "Bond behavior of CFRP bars in simply supported reinforced concrete beam with hanging region." Journal of Composites for Construction 11, no. 2 (2007): 129-137. doi:10.1061/(ASCE)1090-0268(2007)11:2(129).

[4] Elgabbas, Fareed Mahmoud. "Development and structural testing of new basalt fiber-reinforced-polymer (BFRP) bars in RC beams and bridge-deck slabs.". Ph.D. Thesis. (2016).

[5] Panahi, Minu, and Mohsen Izadinia. "A Parametric Study on the Flexural Strengthening of Reinforced Concrete Beams with Near Surface Mounted FRP Bars." Civil Engineering Journal 4, no. 8 (August 31, 2018): 1917. doi:10.28991/cej-03091126.

[6] Sharaky, I.A., M. Baena, C. Barris, H.E.M. Sallam, and L. Torres. "Effect of Axial Stiffness of NSM FRP Reinforcement and Concrete Cover Confinement on Flexural Behaviour of Strengthened RC Beams: Experimental and Numerical Study." Engineering Structures 173 (October 2018): 987–1001. doi:10.1016/j.engstruct.2018.07.062.

[7] Mohsen, Kobraei, Zamin Jumaat Mohd, and Shafigh Payam. "An Experimental Study on Shear Reinforcement in RC Beams Using CFRP-Bars." Scientific Research and Essays 6, no. 16 (August 19, 2011): 3447–3460. doi:10.5897/sre11.650.

[8] Harris, Harry G., Win Somboonsong, and Frank K. Ko. "New ductile hybrid FRP reinforcing bar for concrete structures." Journal of composites for construction 2, no. 1 (1998): 28-37. doi:10.1061/(ASCE)1090-0268(1998)2:1(28).

[9] Zhu, Haitang, Shengzhao Cheng, Danying Gao, Sheikh M. Neaz, and Chuanchuan Li. "Flexural Behavior of Partially Fiber-Reinforced High-Strength Concrete Beams Reinforced with FRP Bars." Construction and Building Materials 161 (February 2018): 587–597. doi:10.1016/j.conbuildmat.2017.12.003.

[10] Alsayed, Saleh H., and Abdulrahman M. Alhozaimy. "Ductility of Concrete Beams Reinforced with FRP Bars and Steel Fibers." Journal of Composite Materials 33, no. 19 (October 1999): 1792–1806. doi:10.1177/002199839903301902.

[11] Ju, Minkwan, Kyoungsoo Park, and Cheolwoo Park. "Punching Shear Behavior of Two-Way Concrete Slabs Reinforced with Glass-Fiber-Reinforced Polymer (GFRP) Bars." Polymers 10, no. 8 (August 9, 2018): 893. doi:10.3390/polym10080893.

[12] Yoo, Doo-Yeol, Nemkumar Banthia, and Young-Soo Yoon. "Predicting Service Deflection of Ultra-High-Performance Fiber-Reinforced Concrete Beams Reinforced with GFRP Bars." Composites Part B: Engineering 99 (August 2016): 381–397. doi:10.1016/j.compositesb.2016.06.013.

[13] Khorasani, A.M. Mohtaj, M. Reza Esfahani, and Javad Sabzi. "The Effect of Transverse and Flexural Reinforcement on Deflection and Cracking of GFRP Bar Reinforced Concrete Beams." Composites Part B: Engineering 161 (March 2019): 530–546. doi:10.1016/j.compositesb.2018.12.127.

[14] ACI (American Concrete Institute) Committee 440, "Guide for the Design and Construction of Concrete Reinforced with FRP Bars," (2015).

[15] G. Karayannis, Chris, Parthena-Maria K. Kosmidou, and Constantin E. Chalioris. "Reinforced Concrete Beams with Carbon-Fiber-Reinforced Polymer Bars—Experimental Study." Fibers 6, no. 4 (December 14, 2018): 99. doi:10.3390/fib6040099.

[16] Adam, Maher A., Mohamed Said, Ahmed A. Mahmoud, and Ali S. Shanour. "Analytical and Experimental Flexural Behavior of Concrete Beams Reinforced with Glass Fiber Reinforced Polymers Bars." Construction and Building Materials 84 (June 2015): 354–366. doi:10.1016/j.conbuildmat.2015.03.057.

[17] Systèmes, Dassault. "ABAQUS 6.12 Theory manual." Dassault Systèmes Simulia Corp., Providence, Rhode Island (2012).

[18] Jian, Li. "Based on ABQUS of Concrete Structure Nonlinear Finite Element Analysis." Advanced Materials Research 756–759 (September 2013): 186–189. doi:10.4028/www.scientific.net/amr.756-759.186.

[19] Tao, Y., and J. F. Chen. "Concrete Damage Plasticity Model for Modeling FRP-to-Concrete Bond Behavior." Journal of Composites for Construction 19, no. 1 (February 2015): 04014026. doi:10.1061/(asce)cc.1943-5614.0000482.

[20] D. Systèmes, "Abaqus 6.12 - Benchmarks Manual. Acedido a 15/12/2014," p. 1137, 2012.